Expanding the Chemical Space of Aryloxy-naphthoquinones as Potential Anti-chagasic Agents: Synthesis and Trypanosomicidal Activity

Nohemí A. Becerra
Universidad Autónoma de Nuevo León: Universidad Autonoma de Nuevo Leon
Christian Espinosa-Bustos
Pontifical Catholic University of Chile: Pontificia Universidad Catolica de Chile
Karina Vázquez
Universidad Autónoma de Nuevo León: Universidad Autonoma de Nuevo Leon
Gildardo Rivera
Instituto Politécnico Nacional: Instituto Politecnico Nacional
Margot Paulino
Universidad de la República Uruguay: Universidad de la Republica Uruguay
Jorge Cantero
Universidad de la República Uruguay: Universidad de la Republica Uruguay
Benjamín Nogueda
Instituto Politécnico Nacional: Instituto Politecnico Nacional
Fabiola Chacón-Vargas
Universidad Autonoma de Chihuahua
Uziel Castillo-Velazquez
Universidad Autónoma de Nuevo León: Universidad Autonoma de Nuevo Leon
Ana F. Elizondo Rodríguez
Universidad Autónoma de Nuevo León: Universidad Autonoma de Nuevo Leon
Sofía Toledo
Pontificia Universidad Católica de Chile: Pontificia Universidad Catolica de Chile
Adriana Moreno-Rodríguez
Universidad Autónoma Benito Juárez de Oaxaca: Universidad Autonoma Benito Juarez de Oaxaca
Mario Aranda
Pontifical Catholic University of Chile: Pontificia Universidad Catolica de Chile
cristian osvaldo salas (✉ cosalas@uc.cl)
Pontificia Universidad Catolica de Chile https://orcid.org/0000-0001-7620-2459

Research Article

Keywords: Trypanosoma cruzi, trypomastigote, epimastigote, aryloxy-naphthoquinones, pharmacophoric analysis, ADME properties

Posted Date: August 4th, 2021

DOI: https://doi.org/10.21203/rs.3.rs-756093/v1

Abstract

In continuation our effort to research the chemical space of aryloxy-naphthoquinones as potential anti-Chagas agents, we synthesized nine derivatives and these compounds were evaluated *in vitro* against the epimastigote and trypomastigote forms of Mexican strains of *Trypanosoma cruzi* (*T. cruzi*). Most of these derivatives are highly active against epimastigote forms (IC_{50} < 1.0 μM) compared to the reference drug benznidazole (Bzn). Then these were evaluated on trypomastigotes, which is showing better potency results than Bzn for compounds **3b** and **3g**. In addition, the cytotoxicity of these compounds was determined on the murine macrophage cell line J774. **3b** and **3i** were the most selective compounds against NINOA trypomastigote and INC-5 epimastigote forms, respectively. Further these compounds also have good oral bioavailability according to theoretical predictions. Finally, we were able to determine optimal substitution patterns using pharmacophoric models. All these results are provided very useful structural information to continue our designing of naphthoquinone derivatives against *T. cruzi*.

Introduction

Chagas disease or American trypanosomiasis is one of the 20 “Neglected Tropical Diseases” (NTD) (WHO, 2020). The disease is caused by *Trypanosoma cruzi* (*T. cruzi*), a protozoan parasite endemic in Latin America. It affects approximately 7 million people and causes more than 10 000 deaths a year [1]. There are two drugs approved for the treatment of this disease, benznidazole (Bzn) and nifurtimox (Nfx) [2]. Both are effective in the early stages of the disease (acute stage), but their efficacy is limited in advanced stages (chronic stage). These drugs also present serious adverse effects and require long-term therapy leading to treatment suspension [3, 4]. Considering the above and the fact the pharmaceutical industry does not invest in research for NTDs, it is great importance to find new alternatives for the treatment of trypanosomiasis. For this reason, many academic research groups are searching for new trypanosomicidal therapeutic alternatives through the design and synthesis of small molecules [5, 6].

Compounds derived from a naphthoquinone scaffold appear to be an interesting alternative for the Chagas disease pharmacotherapy. Lapachol **I** and α-lapachone **II** (Fig. 1) are important naphthoquinone derivatives in nature with trypanosomicidal activity [7, 8]. Considering this background, a library of 2-aryloxy-1,4-naphthoquinone compounds were synthesized by Bolognesi et al. 2-phenoxy-1,4-naphthoquinone **III** (Fig. 1) was the most prominent derivative in this series, with an IC_{50} of 1.70 μM against *T. cruzi* amastigotes [9].

In recent years, our research group has focused on the search for new anti-*T. cruzi* agents containing the structure of the aryloxy-quinone scaffold. Our first approach was through the synthesis of aryloxy-indolequinone derivatives and their evaluation against *T. cruzi* epimastigotes culture. Of these, 6-phenoxyindolequinone derivative **IV** (Fig. 1) showed excellent inhibitory activity in the nanomolar range against Y strain epimastigote (IC_{50} = 20 nM) [10].

In a subsequent article, our group reported the synthesis and trypanosomicidal activity of 2-aryloxy-naphthoquinones, 7-aryloxyquinolinquinones and 6-aryloxy-furonaphthoquinones derivatives [11]. In this work compound 2-(3-nitrophenyloxy)-naphthoquinone **V** (Fig. 1) showed an IC_{50} = 20 nM and a selectivity index (SI) of 625 against J774 murine macrophage cells, which showed low toxicity against non-neoplastic cells. In our last report on aryloxy-naphthoquinones with trypanosomicidal activity, we obtained good results against epimastigote cultures with an IC_{50} = 230 nM for 2-(4-methyl-3-nitrophenoxy)-naphthoquinone **VI** (Fig. 1) [12].

From these results, we observed the presence of an aryloxy group attached to the naphthoquinone core is important for anti-*T. cruzi* activity. Furthermore, we have noticed the addition of a nitro or a methyl group on the aryloxy moiety gives rise to compounds with equal or better trypanosomicidal activity. It remarked that Nfx and Bzn, drugs have been used in the chemotherapy of Chagas disease, have a nitro group in their structure. Interestingly, in 2017 the FDA has approved Bzn as pharmacological treatment for the Chagas disease [13]. Therefore, considering the aforementioned, in this work, we carried out the synthesis of new naphthoquinones (Fig. 1), which was functionalized according to four criteria, to evaluate the effect of these modifications on the trypanosomicidal effect on epimastigote and tripomastigote forms from Mexican strains of *T. cruzi*.

These modifications were: (a) the substitution of the hydrogen atom on C-3 by bromine or chlorine because it has been reported that this change modulates the trypanosomicidal activity on Tulahuén, NINOA, INC-5 and Y strains [14]. In the aryloxy moiety: (b) the substitutions of a nitro group in the aryloxy moiety at *meta* or *para* position; (c) as shown in **VI**, a methyl group at *para* position and *meta* position; (d) a substitution at *para* position by chlorine atom. With these new derivatives, our group expanded the library of compounds with trypanosomicidal activity and contributed to the chemical space of naphthoquinones with anti-Chagasic activity.

Experimental Section

General

Melting points were determined on a Kofler Thermogerate apparatus and were uncorrected. IR spectra were recorded on a JASCO FT/IR-400 spectrophotometer. NMR spectra were recorded, unless otherwise specified, on a Bruker AM-400 instrument using deuterochloroform ($CDCl_3$) or deuterodimethylsulfoxide (DMSO-δ) solutions containing tetramethylsilane as an internal standard. Samples were analysed using an Advion (Itaca, NY, USA) Expression-L mass spectrometer equipped with an electrospray ionization source (ESI). Sample were directly injected (5 µL) using LC-grade methanol as mobile phase. Mass spectrometry analysis was carried out using the following settings: ESI (-) voltage of 2.5 kV, nebulizer gas (N_2) flow: 3.0 L min-1, drying gas flow: 10 L min-1, desolvation line temperature 200°C and heat block temperature 250°C. Analytes were evaluated in Full Scan mode (m/z) 100–1500. Data was acquired by means of Advion Mass Express and processed applying Data Express Software. Thin layer chromatography (TLC) was performed using Merck GF-254 type 60 silica gel. Column chromatography

was carried out using Merck type 9385 silica gel. The purity of the compounds was determined by TLC. All the spectra of aryloxy-quinones synthesized are shown in the Supporting information.

General procedure for the synthesis of aryloxy-naphthoquinones.

In a reaction flask, the suitable phenol (1.1 mmol) and K_2CO_3 (2 mmol) were suspended in DMF (5 mL). The mixture was stirred for 10 min, and then, the corresponding naphthoquinone (1 mmol) was added. Later, the reaction mixture was stirred for 2–3 h at room temperature. The solvent was then removed under vacuum, and the solid residue was purified by column chromatography on silica gel and using dichloromethane as the mobile phase.

2-(4-Methyl-3-nitrophenoxy)naphthalene-1,4-dione 3a. Yellow solid, yield 63 %, mp 163–165°C. ^{1}H NMR (400 MHz, $CDCl_3$) δ 8.21–8.15 (m, 1H), 8.10–8.03 (m, 1H), 7.81 (d, *J* = 2.5 Hz, 1H), 7.79–7.75 (m, 2H), 7.46 (d, *J* = 8.4 Hz, 1H), 7.32 (dd, *J* = 8.4, 2.5 Hz, 1H), 6.01 (s, 1H), 2.64 (s, 3H). ^{13}C NMR (101 MHz, CDCl3) δ 184.48, 179.34, 159.48, 151.07, 149.73, 134.67, 134.63, 133.81, 131.99, 131.82, 130.96, 126.90, 126.38, 125.71, 117.51, 114.42, 20.12. MS (ESI) for ($C_{17}H_{11}NO_5$ [M-]): 309.3. Found 309.0.

2-Chloro-3-(4-methyl-3-nitrophenoxy)naphthalene-1,4-dione 3b. Yellow solid, yield 23 %, mp 201–203°C. ^{1}H NMR (400 MHz, $CDCl_3$) δ 8.22 (d, *J* = 7.0 Hz, 1H), 8.05 (d, *J* = 6.8 Hz, 1H), 7.85–7.74 (m, 2H), 7.61 (d, *J* = 1.6 Hz, 1H), 7.33 (d, *J* = 8.4 Hz, 1H), 7.24–7.17 (m, 1H), 2.58 (s, 3H). ^{13}C NMR (101 MHz, $CDCl_3$) δ 178.02, 177.62, 154.49, 152.74, 149.27, 134.85, 134.67, 134.47, 134.00, 131.16, 130.43, 129.37, 127.58, 127.31, 121.66, 112.82, 20.02. MS (ESI) for ($C_{17}H_{10}ClNO_5$ [M-]): 343.0. Found 343.0.

2-Bromo-3-(4-methyl-3-nitrophenoxy)naphthalene-1,4-dione 3c. Yellow solid, yield 24 %, mp 188–190°C. ^{1}H NMR (400 MHz, CDCl3) δ 8.16–8.08 (m, 1H), 7.95 (dd, *J* = 7.2, 1.7 Hz, 1H), 7.76–7.64 (m, 2H), 7.52 (d, *J* = 2.6 Hz, 1H), 7.24 (d, *J* = 8.5 Hz, 1H), 7.13 (dd, *J* = 8.4, 2.6 Hz, 1H), 2.49 (s, 3H). ^{13}C NMR (101 MHz, $CDCl_3$) δ 178.07, 177.09, 155.21, 154.37, 149.28, 134.81, 134.59, 134.01, 131.06, 130.44, 129.33, 128.61, 127.84, 127.37, 121.64, 112.81, 20.02. MS (ESI) for ($C_{17}H_{10}BrNO_5$ [M-]): 386.9. Found 387.0

2-(4-Chloro-3-nitrophenoxy)naphthalene-1,4-dione 3d. Yellow solid, yield 54 %, mp 164–165°C. ^{1}H NMR (400 MHz, $CDCl_3$) δ 8.18–8.14 (m, 1H), 8.09–8.05 (m, 1H), 7.83–7.74 (m, 2H), 7.72 (d, *J* = 2.8 Hz, 1H), 7.65 (d, *J* = 8.8 Hz, 1H), 7.35 (dd, *J* = 8.8, 2.8 Hz, 1H), 6.11 (s, 1H). ^{13}C NMR (101 MHz, $CDCl_3$) δ 184.25, 179.06, 158.73, 151.80, 148.51, 134.80, 133.97, 133.66, 131.75, 130.88, 126.95, 126.48, 125.68, 124.71, 118.27, 115.61. MS (ESI) for ($C_{16}H_8ClNO_5$ [M-]): 329.0. Found 328.9.

2-Chloro-3-(4-chloro-3-nitrophenoxy)naphthalene-1,4-dione 3e. Yellow solid, yield 43 %, mp 199–201°C. ^{1}H NMR (400 MHz, DMSO) δ 8.14 (dd, J = 7.3, 1.4 Hz, 1H), 8.09 (d, *J* = 2.9 Hz, 1H), 8.02 (dd, *J* = 7.1, 1.7 Hz, 1H), 7.99–7.92 (m, 2H), 7.80 (d, *J* = 8.9 Hz, 1H), 7.67 (dd, *J* = 8.9, 3.0 Hz, 1H). ^{13}C NMR (101 MHz, DMSO) δ 178.47, 177.95, 155.51, 151.95, 148.86, 135.15, 135.01, 134.85, 133.13, 131.94, 131.10, 127.14, 127.00, 122.24, 119.30, 113.43. MS (ESI) for ($C_{16}H_7Cl_2NO_5$ [M-]): 362.9. Found 363.0.

2-Bromo-3-(4-chloro-3-nitrophenoxy)naphthalene-1,4-dione 3f. Yellow solid, yield 67 %, mp 196–198°C. ^{1}H NMR (400 MHz, DMSO) δ 8.18–8.11 (m, 1H), 8.08 (d, *J* = 2.9 Hz, 1H), 8.06–7.98 (m, 1H), 7.97–7.87 (m, 2H), 7.79 (d, *J* = 8.9 Hz, 1H), 7.66 (dd, *J* = 8.9, 2.9 Hz, 1H). ^{13}C NMR (101 MHz, DMSO) δ 178.73, 177.47, 155.39, 154.40, 148.90, 135.08, 134.93, 133.11, 131.83, 131.13, 129.70, 127.38, 127.07, 122.19, 119.17, 113.37. MS (ESI) for ($C_{16}H_7BrClNO_5$ [M-]): 408.6. Found 409.0.

2-Chloro-3-(4-nitrophenoxy)naphthalene-1,4-dione 3g. Yellow solid, yield 61 %, mp 169–170°C. ^{1}H NMR (400 MHz, $CDCl_3$) δ 8.40–8.31 (m, 3H), 8.21–8.15 (m, 1H), 8.00–7.86 (m, 2H), 7.28–7.13 (m, 2H). ^{13}C NMR (101 MHz, $CDCl_3$) δ 177.86, 177.28, 160.65, 152.42, 143.89, 134.98, 134.81, 131.14, 130.33, 127.68, 127.38, 126.04, 116.77. MS (ESI) for ($C_{16}H_8ClNO_5$ [M-]): 329.0. Found 328.9.

2-Chloro-3-(3-methyl-4-nitrophenoxy)naphthalene-1,4-dione 3h. Yellow solid, yield 37 %, mp 170–171°C. ^{1}H NMR (400 MHz, DMSO) δ 8.19–8.10 (m, 1H), 8.06 (d, *J* = 9.0 Hz, 1H), 8.01 (dd, *J* = 7.1, 1.5 Hz, 1H), 7.98–7.87 (m, 2H), 7.38 (d, *J* = 2.5 Hz, 1H), 7.31 (dd, *J* = 9.0, 2.7 Hz, 1H), 2.51 (s, 2H). ^{13}C NMR (101 MHz, DMSO) δ 178.48, 177.94, 159.47, 152.08, 144.56, 136.99, 135.16, 135.02, 134.99, 131.98, 131.06, 127.69, 127.18, 127.04, 119.70, 115.16, 20.46. MS (ESI) for ($C_{17}H_{10}ClNO_5$ [M-]): 343.0. Found 343.0.

2-Bromo-3-(3-methyl-4-nitrophenoxy)naphthalene-1,4-dione 3i. Yellow solid, yield 32 %, mp 174–176°C. ^{1}H NMR (400 MHz, CDCl3) δ 8.27–8.11 (m, 1H), 8.11–7.95 (m, 2H), 7.85–7.71 (m, 2H), 6.94–6.87 (m, 2H), 2.59 (s, 3H). ^{13}C NMR (101 MHz, CDCl3) δ 178.00, 176.87, 158.86, 154.99, 144.74, 137.29, 134.89, 134.69, 131.08, 130.38, 129.07, 127.92, 127.49, 127.46, 119.90, 114.41, 21.27. MS (ESI) for ($C_{17}H_{10}BrNO_5$ [M-]): 386.9. Found 387.0.

Trypanosomicidal effect

T. cruzi NINOA and INC-5 strain epimastigotes were grown at 28°C in an axenic medium (BHI), as previously described [22], and complemented with 5 % foetal bovine serum. Epimastigotes from a 10-day-old culture (stationary phase) were inoculated into 50 mL of fresh culture medium to reach an initial concentration of 1×10^6. Cell growth was monitored by measuring culture absorbance of the culture at 600 nm in an ELISA Epoch reader (Epoch 2 Microplate Spectrophotometer (BioTek Instruments, Inc., Winooski, VT, USA) every day. Before inoculation, the media was supplemented with a given amount of the drug from a stock solution in DMSO (25 mM). The final DMSO concentration in the culture medium never exceeded 0.4 % and the control was run in the presence of 0.4 % DMSO and in the absence of drugs. The percentage of growth inhibition (% GI) and half-maximal inhibitory concentration values (IC_{50}), and parasite growth were followed in the absence (control), and in the presence, of a range of concentrations of the corresponding drug. On day 5, the absorbance of the culture was measured and related to the control. The IC_{50} value was determined as the concentration of drug needed to reduce the absorbance ratio by 50 %. The experiments of each compound were carried out in triplicate; Bzn was used as a reference compound.

Ex vivo **evaluation of INC-5 and NINOA strain trypomastigotes**

CD1 mice, 6 to 8 weeks old, were peritoneally infected with bloodstream trypomastigotes of the INC-5 and NINOA strains, respectively. After 4 to 6 weeks, at the maximum peak of parasitaemia, the parasitized blood was obtained by cardiac puncture using sodium heparin as an anticoagulant. Blood was adjusted to 1 x 10^6 trypomastigotes/mL. In a 96-well plate, 90 µl of infected blood and 10 µl of 1,4-naphthoquinone derivatives or reference drug dilutions were deposited for a final volume of 100 µl per well. Each evaluation was carried out in triplicate. The compounds with the best IC_{50} in the epimastigotes of each strain were evaluated in trypomastigotes of both strains at 20 µM, 10 µM and 5 µM. The reference drug benznidazole was used as a positive lysis control and wells with untreated blood trypomastigotes were used as a negative lysis control; the microplates were incubated at 4°C for 24 h. Subsequently, mobile trypomastigotes were quantified using the Brener-Pizzi method, for this, 5 µL of blood was deposited between a slide and a 13 × 13 coverslip. The trypomastigotes were counted in 15 microscope fields in an optical microscope with 40x magnification. The percentage of lysis of each treatment was calculated by comparing the viable trypomastigotes with the negative control [16]. The LC_{50} was determined by linear regression. The experiments were carried out in accordance with the recommendations and approval of the local Ethics and Research Committee (Approval number: ENCB / CEI / 078/2020).

Cytotoxicity assays

A 96-well plate was seeded with 50 000 cells/well with RPMI medium and 2 % foetal bovine serum and incubated for 24 h at 37°C. The compound from stock was dissolved in DMSO for subsequent serial dilutions with PBS until a concentration in the plate that did not exceed 1 % of DMSO was reached. After 24 h, the culture medium was removed from the plate and fresh culture medium was added together with the compounds reaching a final volume of 100 µl per well. The plate was then incubated for 24 h at 37°C in 5 % CO_2 where the following controls were added: cells with the medium as a positive control; cells without culture medium as a negative control; and last, the reference drug, Bzn at a concentration of 20 µM.

After 24 h of incubation, the cell morphology was observed with a microscope and the MTT viability assay was performed. The culture medium was removed and the MTT solution was prepared and later added to the cells; it was incubated for 1 h and the absorbance was read at 570 nm. The following formula was used to obtain the percentage: % cytotoxicity = (100-(mean number of cells with treatment/cells without treatment) *100) [23].

Pharmacophore

A flexible alignment strategy was used, consisting of the overlap of 3D structures, and minimizing the relative distances between equivalent atoms, including the flexibility for all freedom degrees for all rotatable dihedral bonds. Polar-Charged-Hydrophobic (PCH) of the MOE program was used and evaluated over a centroid position (an averaged position of all atoms relates to the feature). Pharmacophoric features in this scheme are annotated as Aro (aromatic), hydrophobic (Hyd), acceptor hydrogen bonding (Acc), and capacity to bound to metallic centres (ML). Afterward, databases were spotted in groups of

high and low growth inhibition of parasites in epimastigotes or trypomastigotes of INC-5, NINOA, respectively. For each group, a pharmacophore was built, and all features present in a minimum of 60 % of molecules were retained. Finally, all pharmacophores were compared.

Results And Discussion

Chemistry

We synthesized new aryloxy-naphthoquinones by nucleophilic substitution reaction of phenols with halo or dihaloquinones in a basic medium at room temperature (Scheme 1) [12, 15, 11]. These aryloxy-naphthoquinones were obtained from low to moderate yields (23–67%). The chemical structures of the compounds **3a-i** were established based on their spectral properties (IR, ^{1}H-NMR, ^{13}C-NMR and MS). The chemical structures and the yield for the synthesis of **3a-i** are shown in the Table 1.

Table 1
Yields for synthesis of aryloxy-naphthoquinone derivatives

Compound	Structure	Yield (%)
3a	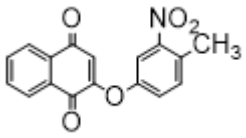	63
3b	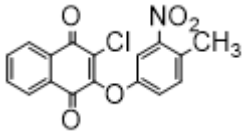	23
3c	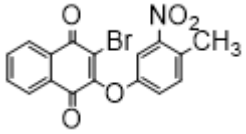	24
3d	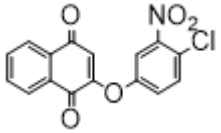	54
3e	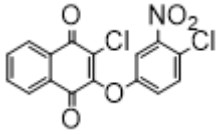	43
3f	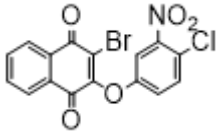	67
3g	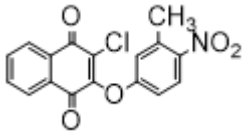	61
3h	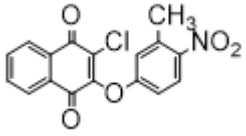	37
3i	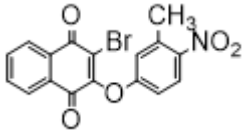	32

Biology

Trypanosomicidal effect against on the epimastigote form

First, a screening assay was performed on the INC-5 and NINOA strains at a fixed concentration of 10 μM to determine the trypanosomicidal effect against epimastigote cultures. The results indicated that all compounds had a percentage of growth inhibition (% GI) in both strains greater than 70%. Considering these results, a dose-dependent assay was carried out using different concentrations (5 μM, 2.5 μM, 1.25 μM, 0.625 μM to determine the half-maximal inhibitory concentration (IC_{50}) in each strain (Table 2).

All the naphthoquinone derivatives showed greater potency than the reference drug Bzn on the INC-5 and NINOA epimastigotes strains. Interestingly, compounds **3i** and **3c** were 1000 and 100-fold more potent than Bzn against the INC-5 strain, respectively. From the chemical point of view, the most active compounds in both strains were **3i** (IC_{50} = 40 nM on INC-5) and **3f** (IC_{50} = 1.14 μM on INC-5). These compounds present a bromine atom at 3-position on the naphthoquinone scaffold. In general, in the INC-5 strain, compounds that have a halogen at 3-position, had greater potency than those did not present a substitution in this position (**3a** and **3d**). The same observation was noticed in the NINOA strain except for compound **3d**, which presented a potency comparable to the derivatives that have halogens at 3-position. On the other hand, the position of the nitro, chloro, or methyl group on the aryloxy moiety does not seem to significantly affect the activity in either strain. However, the halogen attached at 3-position on the naphthoquinone core seems to influence the potency over epimastigotes, since the molecules with a bromine atom were more potent than those with a chlorine atom, and those without substitution in this position are the least active. Therefore, the order of activity follows the pattern: Br > Cl > H.

Table 2
Effect of **3a-i** and Bzn on culture growth of epimastigote and trypomastigote forms of *T. cruzi*

Compound	Epimastigote form		Trypomastigote form	
	INC-5 IC_{50} (μM)[a]	NINOA IC_{50} (μM)	INC-5 LC_{50} (μM)	NINOA LC_{50} (μM)
3a	0.73 ± 0.04	4.86 ± 0.07	NT[b]	NT
3b	0.51 ± 0.02	3.06 ± 0.05	NT	9.38
3c	0.41 ± 0.01	1.70 ± 0.42	24.74	20.35
3d	1.63 ± 0.02	2.26 ± 0.07	NT	NT
3e	0.66 ± 0.01	2.15 ± 0.83	NT	NT
3f	0.88 ± 0.03	1.14 ± 0.03	24.76	20.01
3g	0.64 ± 0.02	1.41 ± 0.05	39.11	9.75
3h	0.67 ± 0.02	1.45 ± 0.03	NT	NT
3i	0.04 ± 0.02	1.84 ± 0.18	27.50	35.36
Bzn	42.3 ± 5.8	8.21 ± 1.8	46.67	40.67

[a]The results are means of three independent experiments

[b]NT = not tested

Trypanosomicidal effect against on the trypomastigote

The half-maximal lytic concentration (LC_{50}) in the trypomastigote form of both strains was measured for the compounds showed the lowest IC_{50} values. The best results were obtained in the NINOA strain with LC_{50} values of 9.38 and 9.75 μM for compounds **3b** and **3g**, respectively (Table 2). These compounds were four-fold more active than Bzn (LC_{50} = 40.67 μM). On the other hand, in the INC-5 strain, two compounds, **3c** and **3g** showed approximately two-fold greater potency than Bzn (LC_{50} = 46.67 μM). However, it was not possible to establish a structure-activity relationship in trypomastigotes because the assayed compounds were limited in number It is remarkable that in NINOA, the most active compounds were those with a chlorine atom at 3-position on the naphthoquinone core.

The important results are obtained from these strains. The trypomastigote is the infective flagellated form of the parasite in the blood. This form is responsible for the acute and chronic stages of Chagas disease in mammalian hosts [16]. Epimastigotes were used as a primary screening because their replication is extracellular, and they are easy to handle and maintain in the laboratory [17].

Cytotoxicity in murine macrophages

The cytotoxicity of the most promising compounds **3b**, **3c**, **3f**, **3g** and **3i** was determined on the murine macrophage J774 cell line (Table 3). In general, the five derivatives had greater selectivity for the epimastigote form of both strains, with **3i** being the compound with the highest selectivity index (SI = 320). Moreover, it is important to point out the high selectivity of compound **3b** against the NINOA strain in trypomastigotes. The SI for **3b** was comparable with Bzn but with a better LC_{50} on this strain than this reference drug.

Table 3
Selective index (SI) values calculated for the most promising compounds

Compound	J774 IC_{50} (μM)[a]	INC-5(Epi) SI[b]	NINOA (Epi) SI	INC-5(Tryp) SI	NINOA(Tryp) SI
3b	117	229	38.2	NT[c]	12.5
3c	9.4	23	5.5	0.4	0.5
3f	13.6	16	12.0	0.5	0.7
3g	11.9	19	8.4	0.3	1.2
3i	12.8	320	6.9	0.5	0.4
Bzn	352	8.3	42.8	7.5	8.7
[a]The results are means of three independent experiments					
[b]SI value = IC_{50} values on J774 cells / IC_{50} or LC_{50} *T. cruzi*					
[c]NT = not tested					

Pharmacophoric elucidation

Compounds were aligned by a flexible alignment technique. This technique overlaps 3D structures minimizing the relative distances between equivalent atoms (in each molecule), including flexibility that allows all degrees of freedom in the rotatable angles, covering all possible dihedral angles. The pharmacophoric model was built using the Polar-Charged-Hydrophobic (PCH) scheme in the MOE program [18]. The model was built with all features present in at least 60% of aligned molecules, resulting in the selection of the following features: Aromatic rings (Aro); Hydrophobic centre (Hyd); Hydrogen bond acceptor capacity (Acc); Metal ligation site (ML), and a combination of these. Some combinations could be defined (Acc&ML). Considering that there are more IC_{50} values for the epimastigote form in both strains, a pharmacophoric model was carried out.

Pharmacophoric models for INC-5 epimastigote T. cruzi **growth inhibitors**

The molecules were classified according to their trypanosomicidal (INC-5 epimastigotes) high or low growth inhibition (Fig. 2); their differential features were also detected. The main difference observed between both groups was sites bound to metals (*meta*-position, red spheres) non-favouring bioactivity. In this place, a nitro group at *meta*-position on aryloxy moiety favoured the desired bioactivity. This change affected the electronic density of the aromatic ring sustaining this group because of the high electronegativity of nitrogen and oxygen atoms of the nitro substituent.

Pharmacophoric models of NINOA epimastigotes T. cruzi **growth inhibitors**

The molecules were classified according to their trypanosomicidal (NINOA epimastigotes) high or low growth inhibition (Fig. 3); their differential features were also detected. In this case, bioactivity (NINOA *T. cruzi* epimastigotes growth inhibition) is favoured with the presence of acceptor groups of metallic atoms at *para* position on the phenoxy group (cyan spheres) and non-favoured when these features are placed at *meta*-position (red spheres).

Physicochemical properties

Drug-likeness properties such as the pharmacokinetic (ADME) and pharmacodynamic (e.g., toxicological) profiles are important during the process of discovery and development process of a drug. These properties are shown the optimization of a leading compound to a successful candidate for pre-clinical stages [19].

ADMET properties are important to determine some chemical descriptors such as the polar surface area (PSA) and the molecular weight (MW) of molecules, which are useful to determine the oral absorption of drugs. Small and hydrophilic molecules are undergoing rapid renal clearance, while large and hydrophobic compounds are undergoing extensive hepatic metabolism and poor absorption [20]. Therefore, finding a suitable hydrophilic-hydrophobic drug balance is a great challenge for medicinal chemists. Thus, to evaluate these properties and predict good oral bioavailability, two sets of rules, Lipinski and Veber, should be followed to make a good prediction [21, 20].

Lipinski's rule of five states that an orally bioavailable molecule should not violate the following criteria: $\leq$ 5 hydrogen bond donors (HBD); $\leq$ 10 hydrogen bond acceptors (HBA); a MW < 500, and a log P-value < 5. On the other hand, Veber et al. described the role of PSA and the number of rotatable bonds as criteria to estimate oral bioavailability. Veber's rule states that the compound to be orally bioavailable, it should have either a PSA $\leq$ 140 Å and $\leq$ 10 rotatable bonds (NRB) or $\leq$ 12 HBD and HBA in total and $\leq$ 10 rotatable bonds. As shown in Table 4, compounds **3a-i** achieved the Drug-likeness criteria described by Lipinski and Veber; therefore, they are expected to have good oral bioavailability.

Table 4
Molecular properties of compounds **3a-i**

Compound	MW (Da)	HBA	HBD	MiLogP	TPSA (A^2)	NRB
Desirable value	≤ 500	≤ 10	≤ 5	≤ 5	≤ 140	≤ 10
3a	309.28	6	0	3.69	89.20	3
3b	343.72	6	0	4.29	89.20	3
3c	388.17	6	0	4.42	89.20	3
3d	329.69	6	0	3.91	89.20	3
3e	364.14	6	0	4.52	89.20	3
3f	408.59	6	0	4.65	89.20	3
3g	329.69	6	0	3.91	89.20	3
3h	343.72	6	0	4.29	89.20	3
3i	388.17	6	0	4.42	89.20	3

MW: Molecular weight; HBA: Number of hydrogen bond acceptors; HBD: Number of hydrogen bond donors; MiLogP: Log P value predicted by Molinspiration (www.https://www.molinspiration.com); TPSA: Topological polar surface; NRB: number of rotatable bonds.

Conclusions

In this study, a set of nine aryloxy-naphthoquinones were synthesised and evaluated *in vitro* and *ex vivo* against the epimastigote and trypomastigote forms in two Mexican *T. cruzi* strains. The trypanosomicidal activity of these compounds against both forms and were better than the reference drug, benznidazole (Bzn). The most promising naphthoquinone derivative is compound **3b** due to its highest trypanosomicidal activity against epimastigotes (INC-5 and NINOA strains) and trypomastigote (NINOA strain) and SI values. From the theoretical studies, important features from pharmacophoric models were identified to develop the more active naphthoquinone derivatives. Predictions about their ADME properties indicated that these aryloxy-naphthoquinones would have good bioavailability.

Declarations

Acknowledgements

C.O.S. thanks to DIPOG project Nº 3913-406-81 and C. E.-B. gratefully acknowledges the financial support from FONDECYT (Research Grant No. 1180292).

Conflict of interest

The authors declare that there is no conflict of interest.

References

1. Organization WH. Available online: https://www.who.int/neglected_diseases/diseases/en/. 2020
2. Zuma AA, de Souza W (2021) Chagas Disease Chemotherapy: What Do We Know So Far? Curr Pharm Des. doi:10.2174/1381612827666210216152654
3. Altcheh J, Moscatelli G, Moroni S, Garcia-Bournissen F, Freilij H (2011) Adverse Events After the Use of Benznidazole in Infants and Children With Chagas Disease. Pediatrics 127(1):e212–e218. doi:10.1542/peds.2010-1172
4. Apt BW, Heitmann GI, Jercic LM, Jotre ML, Munoz CDVP, Noemi HI et al (2008) [Guidelines for chagas disease: Part IV. Chagas disease in immune compromised patients]. Rev Chilena Infectol 25(4):289–292. doi:/S0716-10182008000400008
5. Scarim CB, Chin CM (2019) Current Approaches to Drug Discovery for Chagas Disease: Methodological Advances. Comb Chem High Throughput Screen 22(8):509–520. doi:10.2174/1386207322666191010144111
6. Villalta F, Rachakonda G (2019) Advances in preclinical approaches to Chagas disease drug discovery. Expert Opin Drug Discov 14(11):1161–1174. doi:10.1080/17460441.2019.1652593
7. Boveris A, Docampo R, Turrens JF, Stoppani AO (1978) Effect of beta-lapachone on superoxide anion and hydrogen peroxide production in *Trypanosoma cruzi*. Bioch J 175(2):431–439. doi:10.1042/bj1750431
8. Diogo EBT, Dias GG, Rodrigues BL, Guimarães TT, Valença WO, Camara CA et al (2013) Synthesis and anti-*Trypanosoma cruzi* activity of naphthoquinone-containing triazoles: electrochemical studies on the effects of the quinoidal moiety. Bioorg Med Chem 21(21):6337–6348. doi:10.1016/j.bmc.2013.08.055
9. Bolognesi ML, Lizzi F, Perozzo R, Brun R, Cavalli A (2008) Synthesis of a small library of 2-phenoxy-1,4-naphthoquinone and 2-phenoxy-1,4-anthraquinone derivatives bearing anti-trypanosomal and anti-leishmanial activity. Bioorg Med Chem Lett 18(7):2272–2276. doi:10.1016/j.bmcl.2008.03.009
10. Tapia RA, Salas CO, Vázquez K, Espinosa-Bustos C, Soto-Delgado J, Varela J et al (2014) Synthesis and biological characterization of new aryloxyindole-4,9-diones as potent trypanosomicidal agents. Bioorg Med Chem Lett 24(16):3919–3922. doi:https://doi.org/10.1016/j.bmcl.2014.06.044
11. Vázquez K, Espinosa-Bustos C, Soto-Delgado J, Tapia RA, Varela J, Birriel E et al (2015) New aryloxy-quinone derivatives as potential anti-Chagasic agents: synthesis, trypanosomicidal activity, electrochemical properties, pharmacophore elucidation and 3D-QSAR analysis. RSC Adv 5(80):65153–65166. doi:10.1039/C5RA10122K
12. Espinosa-Bustos C, Vázquez K, Varela J, Cerecetto H, Paulino M, Segura R et al (2020) New aryloxy-quinone derivatives with promising activity on *Trypanosoma cruzi*. Arch Pharm 353(1):1900213. doi:https://doi.org/10.1002/ardp.201900213
13. Jarvis LM (2018) the year in new drugs: fda approvals hit a 20-year high in 2017, with cancer and rare-disease drugs dominating the list of new medicines. Chem Eng News 96(4):25–30

14. González A, Becerra N, Kashif M, González M, Cerecetto H, Aguilera E et al. *In vitro* and *in silico* evaluations of new aryloxy-1,4-naphthoquinones as anti-*Trypanosoma cruzi* agents. Med Chem Res. 2020;29(4):665 – 74. doi:10.1007/s00044-020-02512-9
15. Tapia RA, Salas C, Morello A, Maya JD, Toro-Labbe A (2004) Synthesis of dihydronaphthofurandiones and dihydrofuroquinolinediones with trypanocidal activity and analysis of their stereoelectronic properties. Bioorg Med Chem 12(9):2451–2458. doi:10.1016/j.bmc.2004.01.046
16. Chacón-Vargas KF, Nogueda-Torres B, Sánchez-Torres LE, Suarez-Contreras E, Villalobos-Rocha JC, Torres-Martinez Y et al. Trypanocidal Activity of Quinoxaline 1,4 Di-N-oxide Derivatives as Trypanothione Reductase Inhibitors. Molecules. 2017;22(2). doi:10.3390/molecules22020220
17. Martin-Escolano R, Martin-Escolano J, Ballesteros-Garrido R, Cirauqui N, Abarca B, Rosales MJ et al (2020) Repositioning of leishmanicidal [1,2,3]Triazolo[1,5-*a*]pyridinium salts for Chagas disease treatment: *Trypanosoma cruzi* cell death involving mitochondrial membrane depolarisation and Fe-SOD inhibition. Parasitol Res 119(9):2943–2954. doi:10.1007/s00436-020-06779-0
18. MOE (2013) Molecular Operating Environment 08, Chemical Computing. Group, Inc., Montreal
19. Meanwell NA (2011) Improving drug candidates by design: a focus on physicochemical properties as a means of improving compound disposition and safety. Chem Res Toxicol 24(9):1420–1456. doi:10.1021/tx200211v
20. Lipinski CA, Lombardo F, Dominy BW, Feeney PJ (2001) Experimental and computational approaches to estimate solubility and permeability in drug discovery and development settings. Adv Drug Deliv Rev 46(1–3):3–26. doi:10.1016/s0169-409x(00)00129-0
21. Veber DF, Johnson SR, Cheng HY, Smith BR, Ward KW, Kopple KD (2002) Molecular properties that influence the oral bioavailability of drug candidates. J Med Chem 45(12):2615–2623. doi:10.1021/jm020017n
22. Alvarez G, Varela J, Marquez P, Gabay M, Arias Rivas CE, Cuchilla K et al (2014) Optimization of antitrypanosomatid agents: identification of nonmutagenic drug candidates with *in vivo* activity. J Med Chem 57(10):3984–3999. doi:10.1021/jm500018m
23. Faundez M, Pino L, Letelier P, Ortiz C, Lopez R, Seguel C et al (2005) Buthionine sulfoximine increases the toxicity of nifurtimox and benznidazole to *Trypanosoma cruzi*. Antimicrob Agents Chemother 49(1):126–130. doi:10.1128/AAC.49.1.126-130.2005

Figures

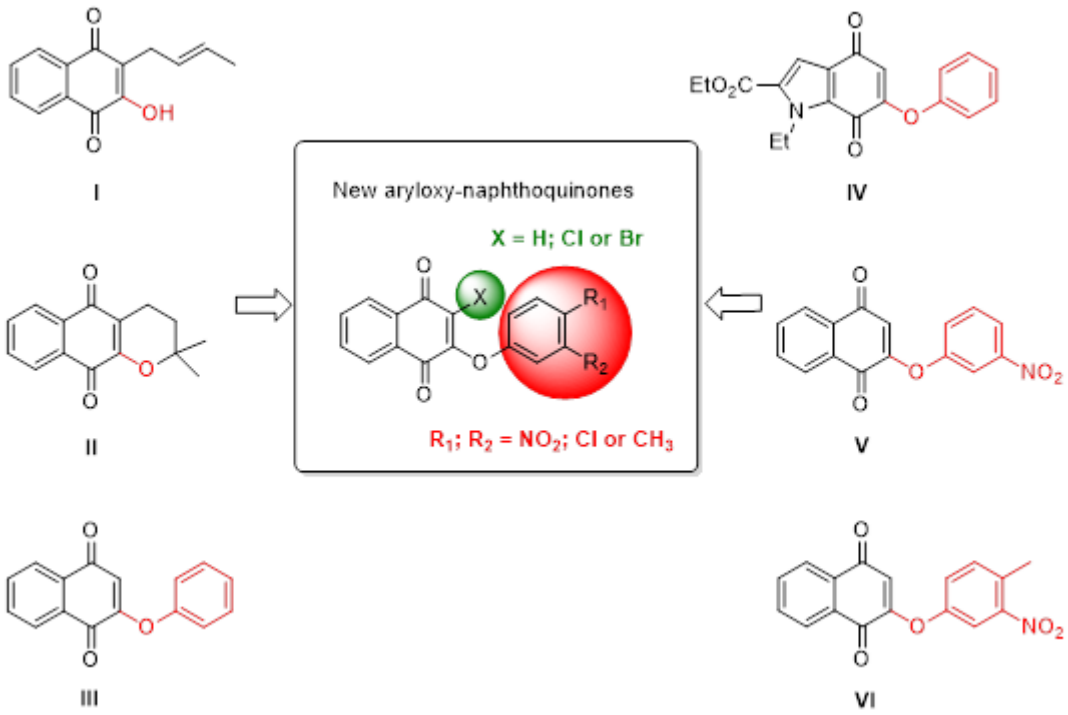

Figure 1

Chemical structures of lapachol (I), α-lapachone (II) and aryloxy-quinones (III-VI) with trypanosomicidal activity, and new aryloxy-naphthoquinones studied in this work

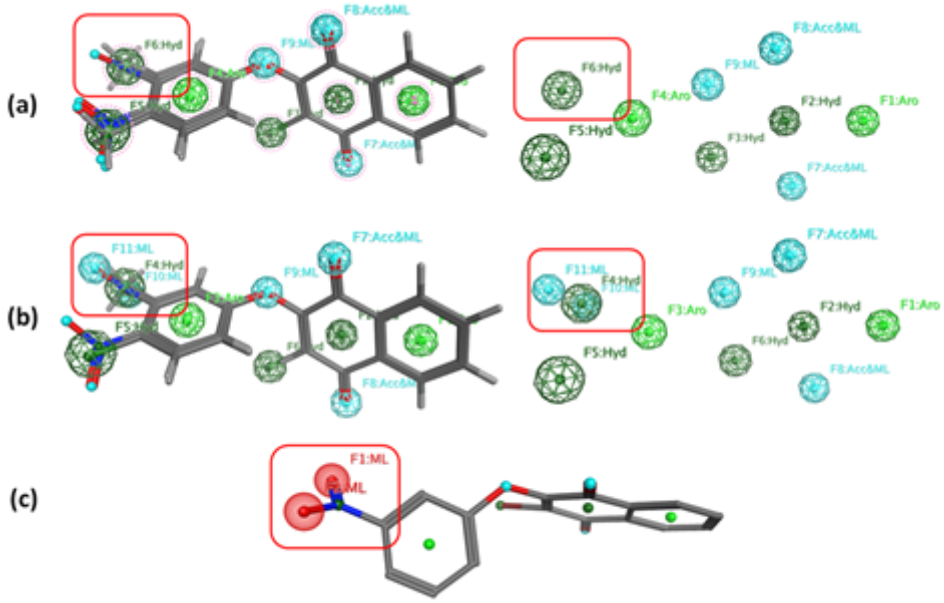

Figure 2

Pharmacophores of molecules with high (a) or low (b) bioactivity and observed differences (c) between both models

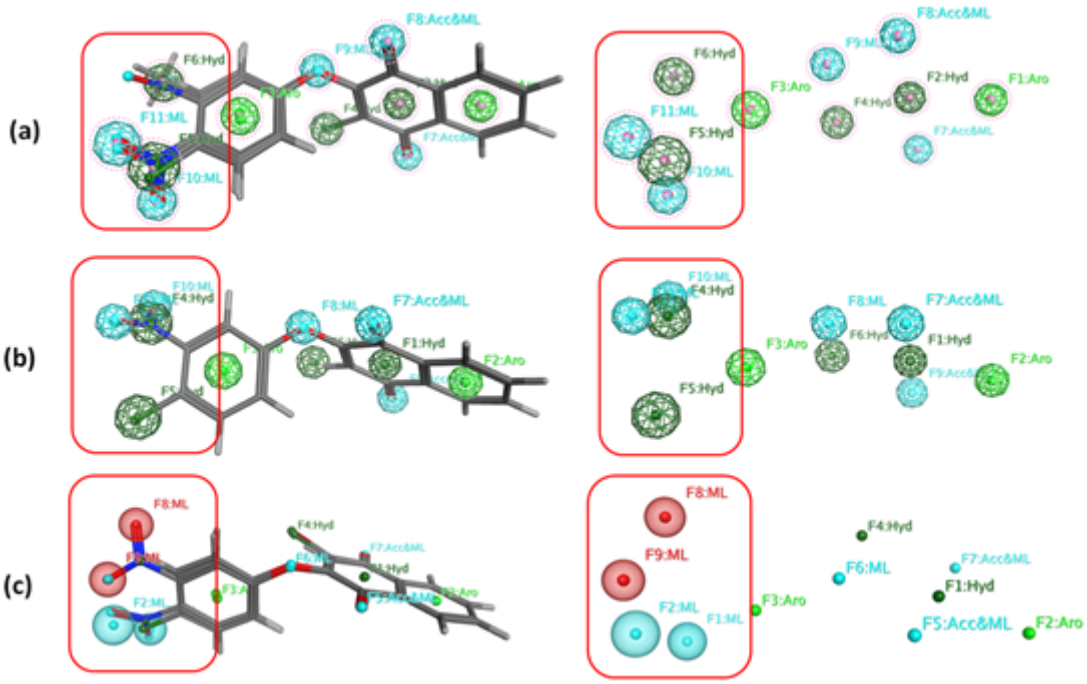

Figure 3

Pharmacophores of molecules with high (a) or low (b) bioactivity (NINOA T. cruzi epimastigotes) and observed differences (c) between both models

Supplementary Files

This is a list of supplementary files associated with this preprint. Click to download.

- SupportinginformationMCR2021.docx
- floatimage1.png
- Scheme01.png